Risø-R-1392(EN)

Full scale testing of wind turbine blade to failure - flapwise loading

Erik R. Jørgensen, Kaj. K. Borum, Malcolm McGugan, Christian L. Thomsen, Find M. Jensen, Christian P. Debel og Bent F. Sørensen

Risø National Laboratory, Roskilde
June 2004

Abstract A 25m wind turbine blade was tested to failure when subjected to a flapwise load. With the test setup, it was possible to test the blade to failure at three different locations.
The objective of these tests is to learn about how a wind turbine blade fails when exposed to a large flapwise load and how failures propagate.
The report shows also results from ultra sonic scan of the surface of the blade and it is seen to be very useful for the detection of defects, especially in the layer between the skin laminate and the load carrying main spar.
Acoustic emission was successfully used as sensor for the detection of damages in the blade during the test.
The report contains measurements of the total deflection of the blade, the local deflection of the skin and the load carrying main spar and also measurement of strain all as a function of the applied load and up to failure of the blade.
The “post mortem” analysis and description of how the damages propagate during the tests are reported in a separate report [2].

ISBN 87-550-3181-1
ISBN 87-550-3183-8(Internet)
ISSN 0106-2840

Print: Pitney Bowes Management Services Denmark A/S

Contents

Preface

This report contains a description of some of the work that was carried out in a project called "Improved design for large wind turbine blades, based on studies of scale-effects (Phase 1)", partially supported by the Danish Energy Authority under the Ministry of Economics and Business Affairs through a EFP2001-fund (journal no. 1363/01-01-0007). The project ran 1½ year from 2001 to 2002. The participants in the project were: The Materials Research Department, Risø National Laboratory (project leader), The Wind Energy Department, Risø National Laboratory, The Department of Mechanical Engineering (Solid Mechanics), The Technical University of Denmark, Department of Mechanical Engineering, Aalborg University, LM Glasfiber A/S and Vestas Wind Systems A/S. It was found to be impossible to acquire students at Aalborg University. As a result, no work was performed there. Instead, more work was carried out at Risø National Laboratory.

This report only contains the results of a full scale test of a 25m Vestas wind turbine blade. The major results of the entire project can be found in the summary-report, which also contains a list of the publications that came out of the project:

Risø-R-1390(EN)
"Fundamentals for improved design of large wind turbine blade of fibre composites based on studies of scale effects (Phase 1) - Summary Report" , Bent F. Sørensen, Erik Jørgensen, Christian P. Debel, Find M. Jensen and Henrik M. Jensen, ISBN 87-550-3176-5; ISBN 87-550-3177-3(Internet) ISSN 0106-2840

1 Introduction

The purpose of the test was to obtain detailed information about failure mechanisms in a wind turbine blade, especially with focus on failures in the compression side of the blade.

Prior to the tests the blade was inspected by means of an ultra sonic test to get an overview of imperfections and damages already present before starting the test. This test was verified and supported by a simple, so-called tap test.

The supports and loading procedure of the blade was done in a way making it possible to use the same blade in three failure tests, i.e. having independent failures in three different sections of the blade.

During each of the tests the damages were surveyed and measured by means of video and photos, strain gauges, acoustic emission and deflection sensors. Two different types of deflection sensors were mounted on the blade, one giving the total deflection of the blade and another giving skin and main spar displacements, locally. Each test was stopped at every sign of damage and inspected visually. Cracks and propagation of the damages were identified. A simple tap test was also done to identify the propagation of delaminations.

Finally, after the collapse of the blade, the failures and failure mechanisms was investigated, the results from this study are reported in "Indentification of Damage Types in Wind Turbine Blades Tested to Failure" [2].

2 Blade

The blade used in the tests was a 25m blade (V52), which was supplied by Vestas as part of the project. The blade is an epoxy glass fiber (prepreg) blade.

Prior to this test, this specific blade was tested in a static test to prove the overall strength, actually as part of the design approval of the blade type [1], i.e. the blade had already been loaded to the design load and afterwards tested with the design fatigue loads which are similar to 20years lifetime. This blade passed both the tests. Because this blade already had been loaded heavily, internal damages could be present before starting the test covered in this report. Therefore an ultra sonic test and a tap test was carried out to investigate if any damage was present

2.1 Definitions

The test program consists of three tests, making it possible to study, independent failures in three different sections of the blade. The three sections were chosen on the basis of complexity and differences of the geometry and the calculated strength of the blade.

The three test sections were named as “section 1”, “section 2” and “section 3” and these as well as the coordinate system used in the tests are shown in the figures below.

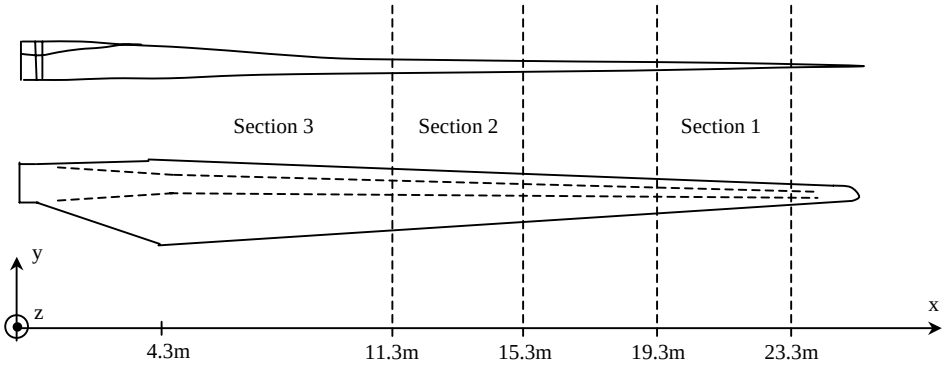

Figure 1 Definition of test sections and co-ordinate system (coordinate system is related to the lower drawing, i.e. with the aerodynamic suction side upwards)

The x-axis is along the blade, starting at the root end of the blade as indicated on the figure above. The y-axis is in the chordwise direction, positive towards the leading edge. The z-axis is positive in the direction of the wind. Actually when measuring the distances on the blade, a local coordinate system is used, as seen in the figure below. Here the y-value is taken as the curve length starting at the trailing edge and positive towards the leading edge.

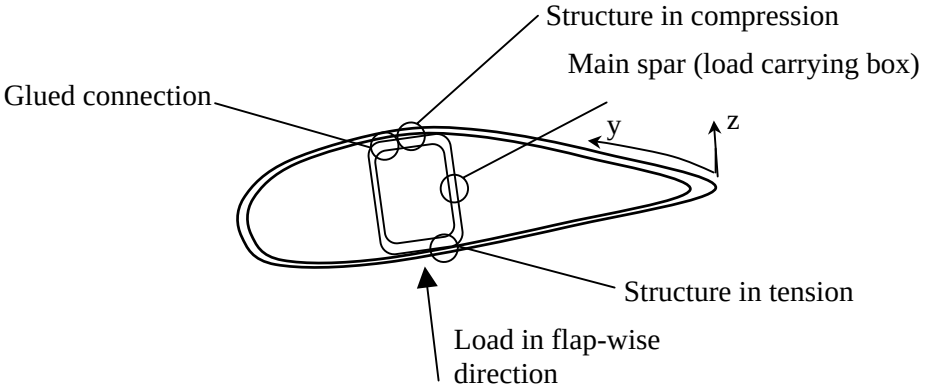

Figure 2 Sketch of section of blade (Local coordinates)

3 NDT of blade

3.1 Ultra sonic test

Before starting the tests an ultra sonic test was carried out in the areas of the three test sections to verify if any damages, because of the history of the blade, or imperfections from the production of the blade, were present in blade and therefore could be expected to initiate damage. The Danish institute "FORCE Technology" carried out the ultra sonic test.
The width of the scanned zones was 0.5m and covering the area over the main spar. Only the compression side of the blade (see figure 2) was investigated by means of the ultra sonic tests. The tested areas had a length of 3.6m, 3.6m and 6m. This covered section 1, section 2 and section 3 as given in figure 1.
A mobile scanning system, with two transducers, was mounted on the blade with suckers. The resolution/steps of the scans was 2.5mm. The ultra sonic waves are transmitted to the blade through water and the reflections from inter-faces like skin to glue, glue to main spar were measured. If any delaminations or lack of glue is in the zone, reflections will also been seen from these.
In the figure below the result of such a scanning of the blade sections 3 are shown.

In the scanning of the three sections the following symbols and explanations was given by FORCE Technology. Some of the explanations are not relevant for the actual section shown in this figure, but relevant for other sections.

i1: Skin/glue
In this area a red color indicates bad cohesion between skin laminate and epoxy or missing epoxy.

i2: Glue/main spar
In this area a yellow/green color indicates no cohesion between glue and main spar

i3: Delamination in laminate in main spar
In this area a yellow/green color indicates delamination in laminate in main spar

g1: Sandwich
Transition from red to yellow/green color indicates borders of the foam towards trailing edge.

g2: Sandwich
Transition from red to yellow/green color indicates borders of the foam towards leading edge.

c1: Tranducer signal not good
This area could not evaluated

o1: Area with damping
Blue color indicates high damping in skin or main spar laminate, which could be caused by porosities

o2: Damping in skin
Blue color indicates high damping in skin, which could be caused by porosities or more likely change of thickness of laminate.

The figure below shows the result of an ultrasonic scan of section 3.

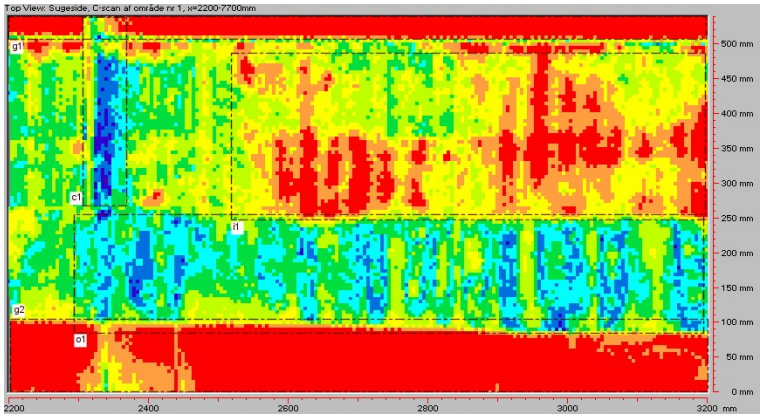

Figure 3 Ultrasonic scan from 2.2m to 3.2m (section 3)

In this scan a good adhesion between the layers is seen, even though there are areas (marked i1, red), which indicates missing adhesion or epoxy.
In this scan red ”lines” are seen in upper right part of the figure, which indicates how the epoxy is put in lines during manufacturing of the blade. In other areas these lines where much more dominant and larger areas with a bad adhesion/distribution of epoxy was also seen in some areas.

3.2 Tap test

A simple tap test was carried out to verify and as a supplement to the ultra sonic test. The method is based on the fact that the sound emitted when knocking on the structure changes when the thickness or material type changes or when porosities are present. It could also be caused when the skin laminate debonds from the main spar.

The procedure used was completely manual, that is using a hammer and listening, with the human ear, to the frequency of the sound emitted. Based on the measurements lines were drawn to indicate where debonds were observed. The tap test verified the results from the ultra sonic test and it is a good method to discover irregularities in the structure.

Tap tests were done several times during the tests to see how the debonded areas developed during the test. This is not reported here.

3.3 Acoustic emission

Acoustic emission (AE) from the blade was measured during the test to identify failures and locations of the damages in the blade.

AE sensing was the most effective technique used to immediately (during loading) indicate the location and onset of damage. This allowed the investigation into the causes and growth of the various damage types to be more efficiently controlled by the test operatives. The AE data also warned of unwanted damage such as localised crushing at loading points.

Feedback from the sensors gives the controller more confidence when applying loads during a one-off structure test. This is because he has an improved feeling for how the blade is responding and how close it may be to failure. The probability of an invalid test due to, for example, crush damage at loading yokes is greatly reduced. The occurrence of unexpected damage is more likely to be detected and conducting structure inspections between loadings is made simpler. Various structure specific damage types can be identified as loading takes place.

Processes such as cracking, deformation, debonding, delamination, rubbing, impacts, crushing, turbulence and others, all produce localised transient changes in stored elastic energy with a broad spectral content. Acoustic emission sensors detect the high frequency component of the elastic waves (or stress waves) naturally generated by these energy loss processes within materials and structures.

The AE sensor used in this test was the PAC (Physical Acoustic Corp.) R15I, these sensors are resonant at 150kHz and contain an integral preamplifier.

Two separate systems were used to record the AE activity during the testing:

- A PAC SPARTAN AT system recorded the waveform characteristics of each detected AE signal (amplitude, rise-time, energy, etc.) on two channels.
- A customised system developed by Demex and Risø National Laboratory using LABVIEW Virtual Instruments and based around a high speed data card digitised the entire AE signal waveform detected on four channels.

Both systems could detect a 0.5mm Hsui-Nielsen leadbreak up to 2m from the sensor along the central loading spar and were sensitive to precursor “micro-damage” AE events at the very early stages of the test. These are the kind of

events that create no damage later visible to standard NDT inspection techniques. The SPARTAN was especially effective at generating real-time graphs displaying energy release rates that can be used to highlight the onset of serious “macro-damage” following the precursor “micro-damage”. “Macro-damage events are friction dominated and produce effects which can be later detected by standard NDT inspections. The LABVIEW used a time-of-flight Virtual Instrument that highlighted how AE events, even those emitted at relatively low load levels, clustered around the eventual failure points.

Attaching sensors for these short duration static tests was done simply and quickly using tape and a standard ultrasonic couplant gel to improve contact with the surface. This permitted rapid deployment of the sensors and redeployment when moving on to test the next section of the blade. The LABVIEW sensors were positioned at areas of the blade where bending moment calculations predicted structure failure. The SPARTAN sensors were used to record the general activity levels in key areas, in order to help predict break point. These sensors were also used to check activity levels at loading yokes, warning of any unwanted crushing damage for example.

4 Experimental procedure

Three different tests, to a complete failure of the blade, were carried out. By using different supports on the blade this was made possible herbeby giving the opportunity to investigate three independent failures in only one blade. The sections tested, were decided based on knowledge of calculated compression strength and the blade geometry. One difficult task was then to find out how to load and support the blade so that the failures happened in these regions and not near the yokes for support and load inputs.

The calculated design strength of the blade was known from the manufacturer and the task was then to achieve a distribution of the bending moment (M) in the blade to have the damage in a desired region.

The three different test setups, showing where the loads and supports were put to get the failures at the predetermined locations, are shown in Figure 4 to Figure 6. Especially in test of section 2 it was required with a more complex loading setup to have the failure, at least according to the strength calculations, at the chosen location.

The comparison of the calculated design strains with the calculated distribution of strain (using a simple FE 3D-beam model) with the loads during the tests, it was found that the blade most probably would fail for section 1 at 20.3m from the root, for section 2 in 11.5m from the root and for section 3 in 4.3m from the root. Especially in section 2 the calculated strain and the design strain were very close, over the whole section, and actually the blade could fail at any location from 11.3m to 16m. Most probably close to the 11.3m chord.

During the tests the structural behavior of the blade was monitored with many sensors. The load was measured with a load sensor, directly at the point of load application. The global deflection was also measured at the location of the load. Locally, the skin deflections were measured, in the test section, at five locations. Strain measurements were done along the blade and also inside the main spar. More than a hundred strain gauges were mounted on the blade to give the axial strain. In case of no linearity between deflection/strain and the load the test was stopped and the blade inspected for any damages.

Thus, each test section was subjected to a number of loading and unloading sequences, each time with an increasing peak load, only the last loading sequence, i.e. just before failure of the blade, is shown in this report.

Acoustic emission of the blade was measured during the test to identify failures and locations of the damages in the blade.

Furthermore the test sections were under constant surveillance via two remote controlled video cameras. The video sequences were recorded on a standard VCR.

4.1 Loads and supports

The three different test setups, showing where the loads and supports were put to get the failures in the predetermined sections, are schematically shown in Figure 4 to Figure 6.

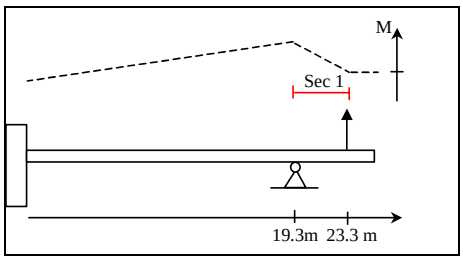

Figure 4 Supports and load inputs in the test of section 1

During all the tests the force was measured with load cells at the point of load application.

In test of section 1 the load in flapwise direction was applied at 23.3m and the support (simple supported) was located at 19.3m to prevent deflections in the flapwise direction.

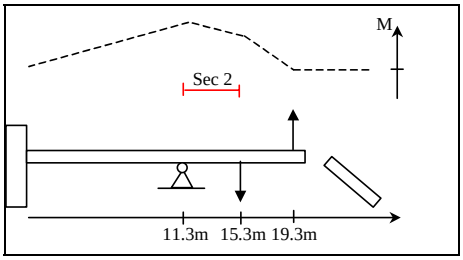

Figure 5 Supports and load inputs in the test of section 2

In test of section 2, it was required with a more complex load and support setup to have the failure at the expected location. Forces were introduced at 19.3m and 15.3m and the support to prevent deflections in flapwise direction was located at 11.3m. By introducing two forces it was possible to change the shape of the bending moment curve by changing the ratio between the two forces. This could be necessary if during the test measurements showed that the failure not was going to happen in the decided section. But even with this sophisticated load setup unfortunately the failure happened very close to the yoke.

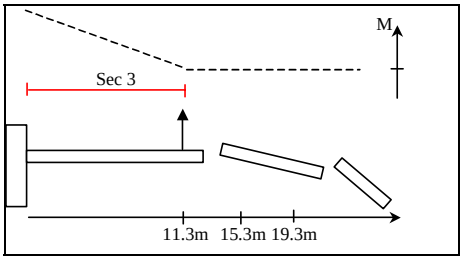

Figure 6 Supports and load inputs in the test of section 3

The setup for test 3 was simpler as only one force was applied at 11.3m.

4.2 Sensors

Full description of the load and deflection sensors as well as the strain gauges are given in [4]

5 Test results

The results of the three test setups are given in this chapter. The data measured during the tests includes beside the load applied, the deflection of the blade, the local deflection of the main spar (as defined in chapter 4.3) and the strain at several locations.

In test of section 1 (19.3m to 23.3m) the blade failed 20.1m from the root, with a load introduction as given in figure 4. In the figures below the large deflection in this test is seen as well as a picture of the failed section of the blade.

Figure 7 Test of section 1, large deflection is seen in this test.

Figure 8 The blade failed 20.1m from the root section. AE sensors where mounted very close to the failure

In test of section 2 the blade failed 15.3m from the root (unfortunately at the yoke), with a load introduction as given in figure 5.

Figure 9 In test of section 2 the blade unfortnunately failed at the loading yoke at 15.3m from root section

In test of section 3 the blade failed 4.4m from the root, with a load introduction as given in figure 6.

Figure 10 Test of section 3 with load introduction at 11.3m

Figure 11 Failure 4.4m from the root.

A comprehensive description and evaluation of the fractures and the development of cracks during the tests are described in [2].

All load values in this report are normalized with one value, i.e. all load values are divided by the same number (which is the overall maximum load during all the tests) to ensure confidentiality.

5.1 Global deflections

The global deflection of the structure was measured during the tests of the three sections. The deflection was measured close to the point of application of the load.
All measured deflection values in this report are also normalized with one value, i.e. all deflection (global and local) values are divided by the same number (which is the maximum global deflection during all the tests) to ensure confidentiality.

The global deflection is not very sensitive to the damages that happen locally and it is very difficult to give any criteria based on the global deflection about how close the blade is to failure. In the figures 12 and 13 the global deflection is given for test of section 1 and 3 and non-linearity is seen in both the figures that could indicate damages in the blade or local buckling. Actually in figure 12 the blade is getting stiffer for higher loads, which does not indicate any damages but the fact that because of the large deflections, the load alone is not enough to give an exact measure of the load (bending moment) applied. With these large deflections the load is not perpendicular to the blade and the angle at which the load is acting have to be taken into account.

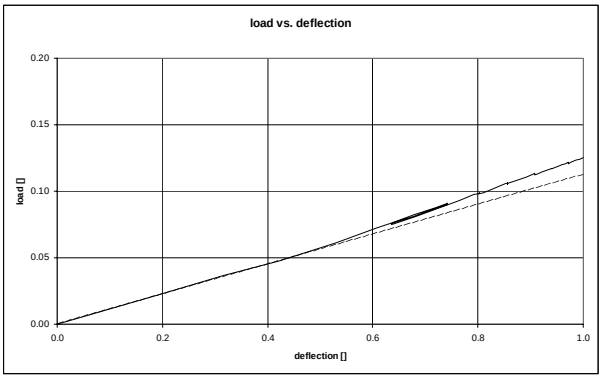

Figure 12 Load vs. deflection during the test of section 1 until fracture (load applied at 23.3m and deflection measured at 23.1m)

Even though the effect, which is much smaller in test of section three than in section one (because of the size of the deflection), a non-linearity is seen in figure 13. In this figure the blade gets more flexible with increasing load and therefore it is indicating "real" non-linearity in the blade (structural or material damage). It is seen that compared to the initial stiffness the blade is approximately 5% more flexible at full load, i.e. load at which value the blade failed.

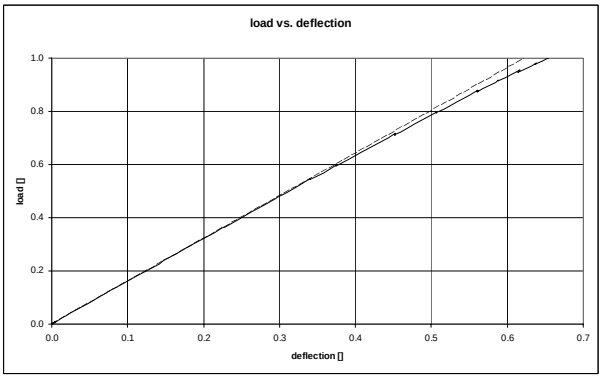

Figure 13 Load vs. deflection during the test of section 3 until fracture (load applied at 11.3m and deflection measured at 11.1m)

5.2 Local deflections

Local deflections were measured on the skin, that is the deflection on the middle of the main spar relative to the webs of the main spar. In flapwise loading the webs are following the blade deflection so placing the measurement system fixed over the two stiff webs of the main spar and then measuring the deflection in the middle of the main spar gives the local deflection of the flange of the main spar as shown on the figure below.

This local deflection was shown to be a good quantity for describing the state of the blade, i.e. how close the blade is to a failure (buckling of the flanges and webs) [3].

The sensors for measuring local deflections were developed during this project.

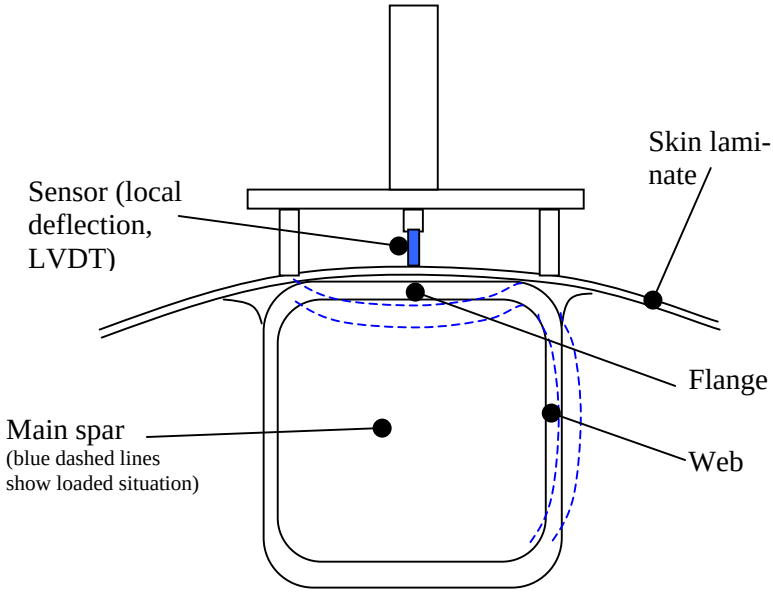

Figure 14 Sketch of the system for measuring local deflections on top of the main spar

A measurement setup including five sensors for measuring local deflections are shown in the figure below for the test of section three.

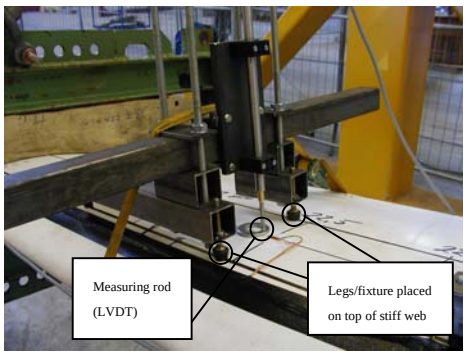

Figure 15 System for measuring local deflections

Figure 16 Local deflection sensors setup for test of section 3

The results of the measurements of the local deflections together with the global deflection are shown, for test of section 3, in the figures below. The data includes all data during the final loading until the blade broke at 4.4m.

All measured deflection values in this report are normalized with one value, i.e. all deflection (global and local) values are divided by the same number (which is the maximum global deflection during all the tests) to ensure confidentiality.

The local deflection at 4.3m is shown in figure 20 and it is seen this curve that it is close to a not stable situation, i.e. the deflection is increasing even though there is no increase in the load.

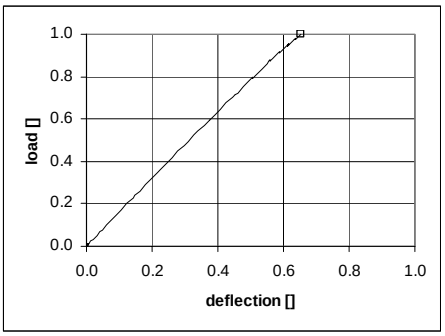

Figure 17 Global deflection of blade measured at 11.1m, load at 11.3m

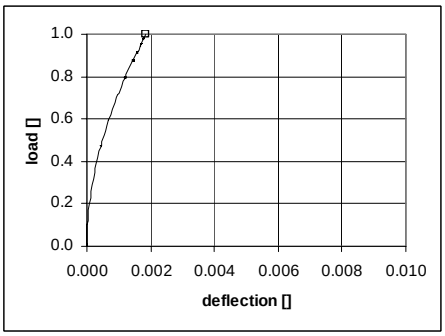

Figure 18 Local deflection at 2.9m, load at 11.3m

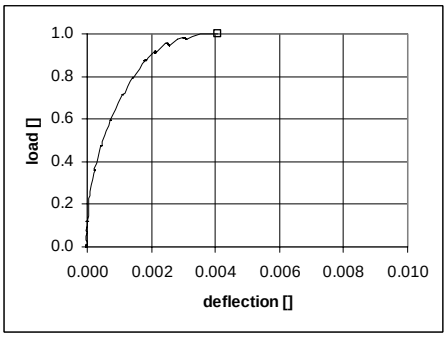

Figure 19 Local deflection at 4.1m, load at 11.3m

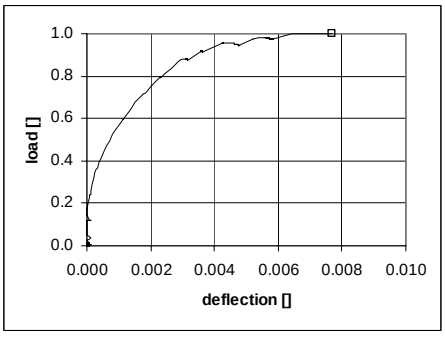

Figure 20 Local deflection at 4.3m, load at 11.3m

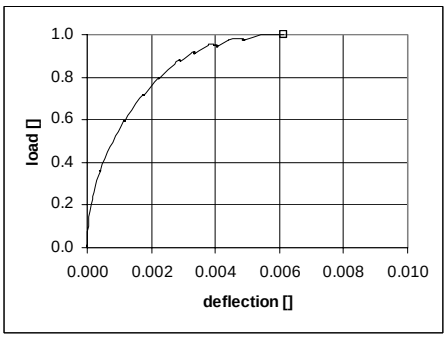

Figure 21 Local deflection at 4.5m, load at 11.3m

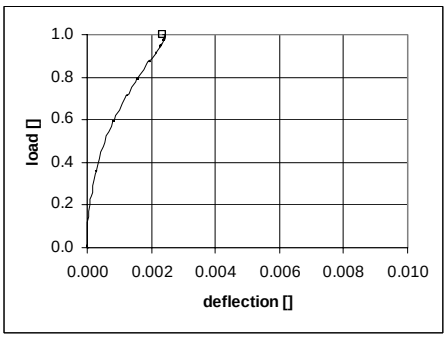

Figure 22 Local deflection at 5.3m, load at 11.3m

This local deflection was shown to be much better to identify how close you are to a failure. Data from all three tests are reported in [4].

5.3 Strain gauge measurements

During the tests the blade was instrumented with strain gauges measuring the strain in the axial direction (lengthwise relative to blade). In all three test sections one strain gauge was placed for every 20cm measuring the strain on the middle of the main spar in the direction of the blade (x-direction, see figure 1) on the external surface of the blade. For every 1.2m strain was measured at four locations, in the middle of the flange (.1) over the webs (.2 and .3) and on the tension side (.4) as shown on the figure below. The numbering system of the strain gauge is so that the first three digits gives the distance from the root in decimeters and the number after the "dot" gives the location according to the figure, example "207.1" means the strain gauge is located 20.7m from the root and the strain is measured on the skin over the middle of the main spar.

To ensure confidentiality all strain values in this report are normalized with one value, i.e.all strain values in this report are divided by the same number.

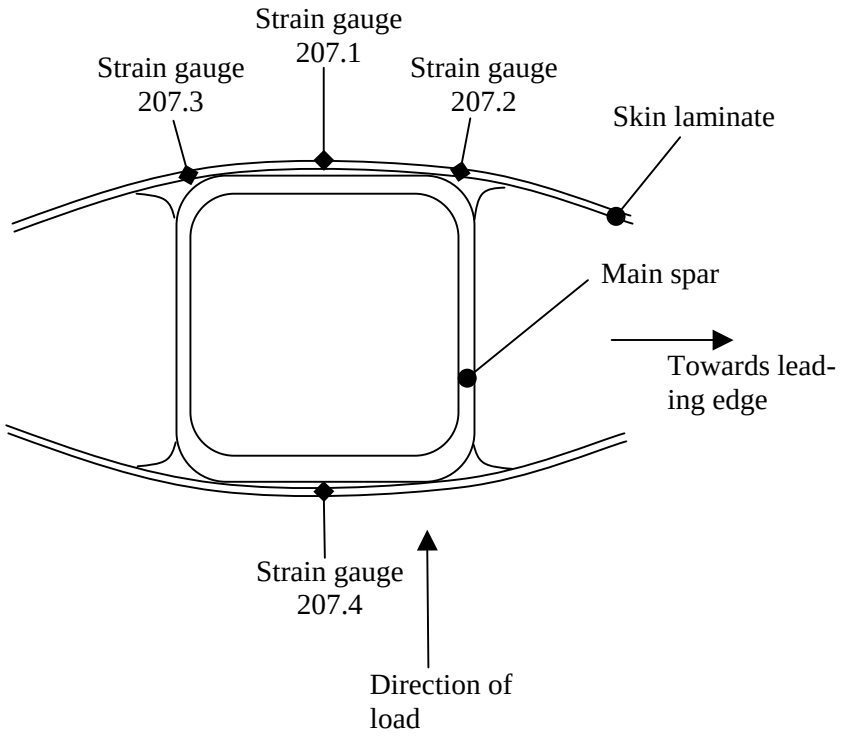

Figure 23 Location of strain gauges, example here given for a section 20.7m from the root section

A typical strain versus load plot is shown in the figure below during the test of section 1. It is seen that during the test the blade is partially unloaded from a level of approximately 0.09 to 0.07 and then loaded up again resulting in the small loops.

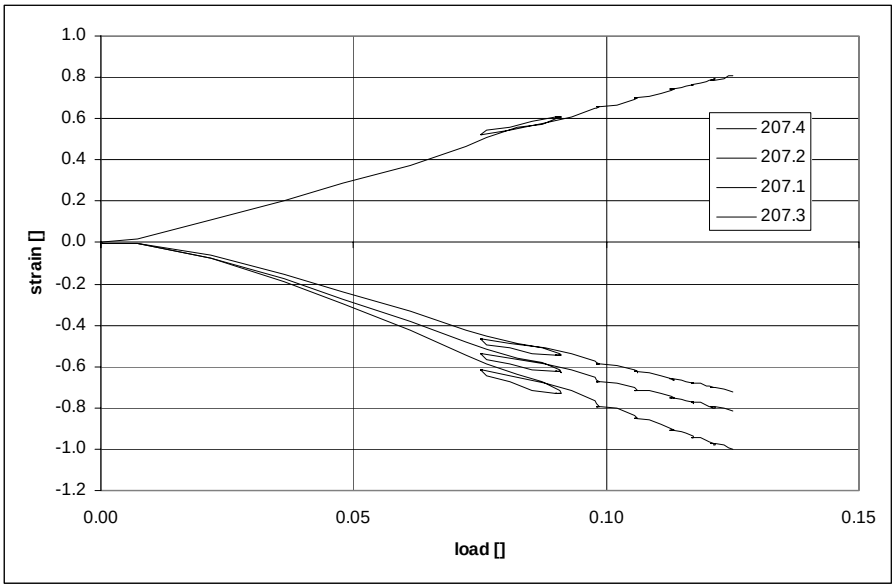

Figure 24 Strain gauge measurement during test of section 1, given at 20.7m form root section

At a specific spot on the blade in test section 1, the skin is visually observed to be buckling. The strain gauges in this area, showed at the same time very high compressive and tension strains. According to figure 27 the strain gauge located on the top of the buckling wave (strain gauge #201.1) showed tension and in the bottom (strain gauge #199.1) showed compression as expected. The area of this debonding of the skin laminate, indicated by the strain gauge measurements as well as seen visually, was corresponding very well with the areas of improper bonding as found in the ultra sonic measurement prior to the test. It should be mentioned that the skin laminate is only a minor part of the load carrying part in a flapwise load situation. The results are shown here for the good correlation between strain gauge measurements, the visual identification and the prediction of the bonding situation based on the ultra sonic test of this area. Even though the skin only contribute as a minor part to the strength of the blade in a flapwise load situation the blade actually failed in this area of delamination (20.1m from the root section).

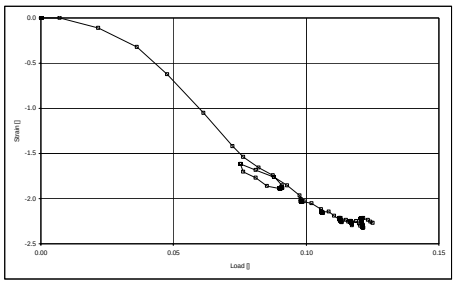

Figure 25 Strain gauge measurements at 19.9m (strain gauge #199.1)

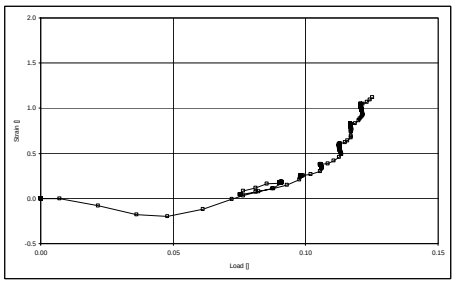

Figure 26 Strain gauge measurements at 20.1m (strain gauge #201.1)

Figure 27 Photo of skin behavior (skin laminate debond from the main spar)

During test of section 3, the blade failed at 4.4m close to the largest chord. In the figure below the strain is shown as function of the load for the strain gauges located in the area of where the failure happened. The strain is seen to be non-linear especially for strain gauge “45.1” which is close to the location where the blade finally failed.

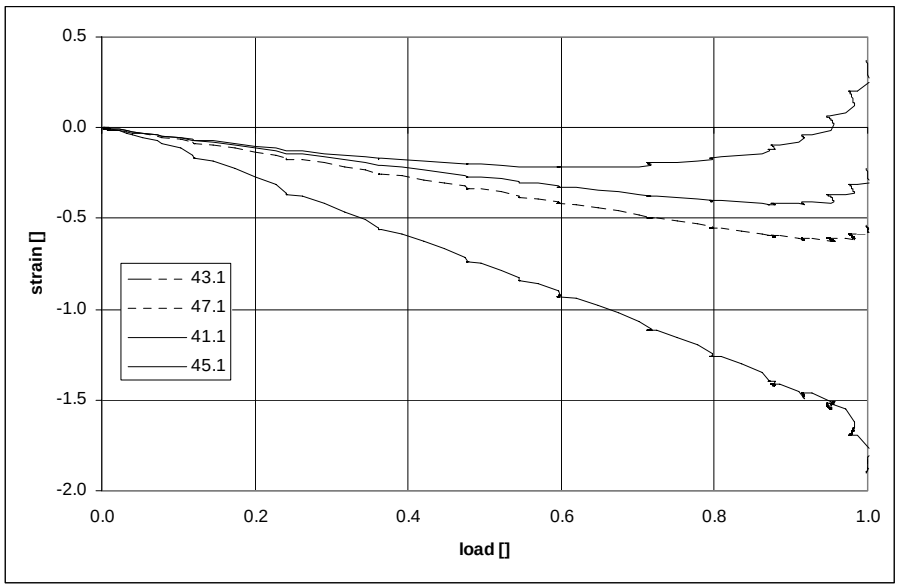

Figure 28 Measured strain on four locations during test of section 3, showing non-linear behaviour

The strain measurements nearest to the root section are seen to be linear, i.e. there is no indication of any failures propagating in this region.

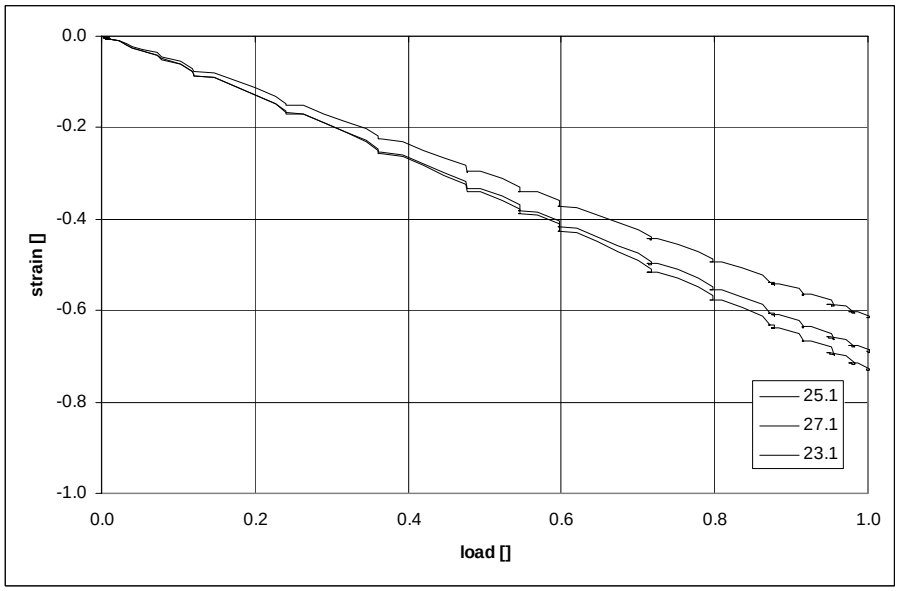

Figure 29 Measured strain on three locations during test of section 3, showing linear behaviour

5.4 Acoustic emission

For test section 1 the LABVIEW sensors were positioned at 20.1m in the area of predicted failure on the compression face in order to generate a location plot of significant AE activity. The SPARTAN sensors were used to compare the level of activity at the 19.3m loading yoke with the activity at the 20.1m chord.

A LABVIEW system location plot was generated from data sampled during loading up to 77% of the load at failure. This plot corresponded exactly with the failure that occurred during a subsequent loading.

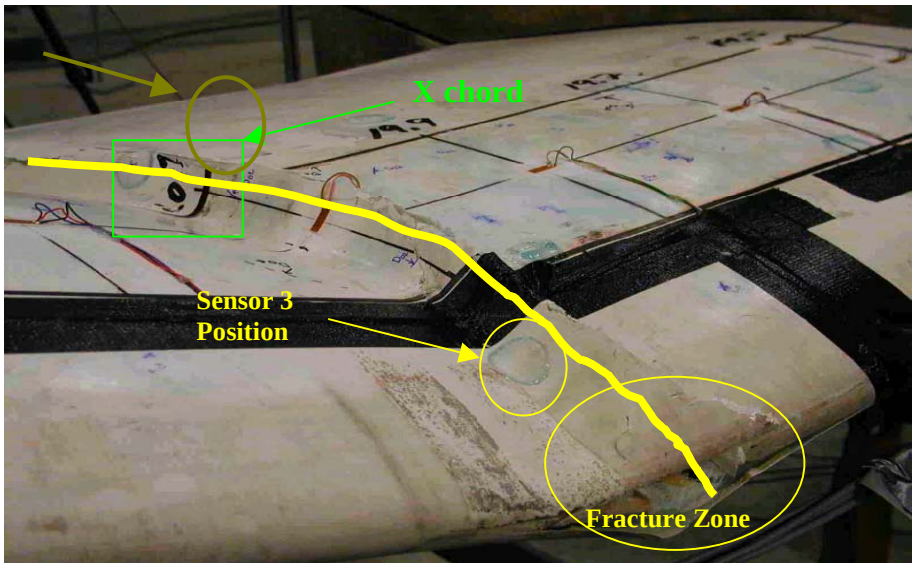

Figure 30 Blade failure at the 20.1m chord. Note position of sensor 3

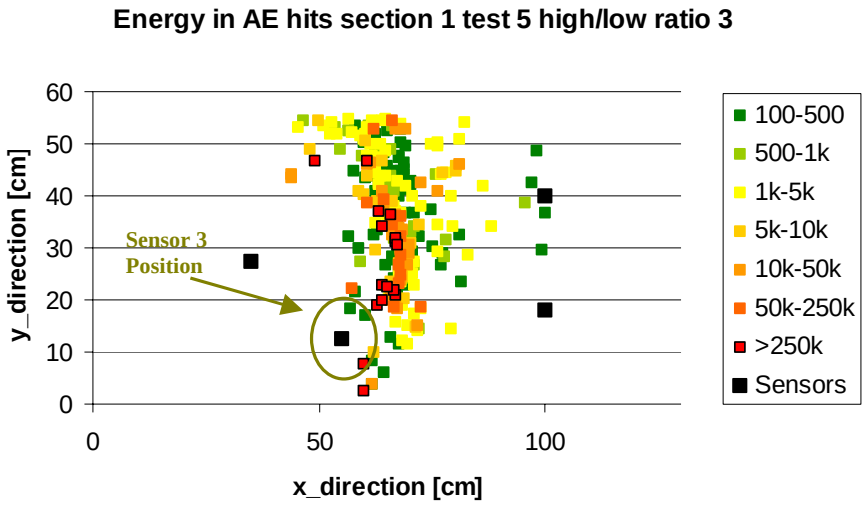

Figure 31 LABVIEW system localisation of AE events prior to failure. High activity events distributed along ultimate failure chord. Note position of sensor 3.

The SPARTAN system displayed the cumulated AE activity levels at both the loading yoke and the predicted failure chord in real time. As the vast majority of activity was detected at the predicted chord, this gave a visual indicator to the test operatives that the loading was proceeding as expected and that no unwanted damage types were occurring.

As mentioned previous a slightly more complex loading setup was used to test blade section 2. The strength calculations predicted failure around the 11.5m to 12m chord of the blade. However, the LABVIEW location sensors positioned here registered almost no activity during step-wise loading. By comparison the SPARTAN guard sensor (sensor 2), which had been positioned at the 15.3m loading yoke, successfully warned, very early in the test, that failure would in fact occur here.

In the first loading sequence for this test section there was an accumulated stress wave energy count of 16000 recorded at SPARTAN sensor 2, positioned as a guard at the 15.3m loading yoke. By comparison there was only 700 recorded at SPARTAN sensor 1 positioned at the 11.3m clamping yoke, far closer to the desired failure chord. At a load cell voltage of 3.63V, it was suggested, by the AE operatives, that the load should be released and the blade inspected. This was due to a rapid increase in the activity level for SPARTAN sensor 2 during the load increase to 3.63V, followed by an extremely long period during load hold where AE activity continued.

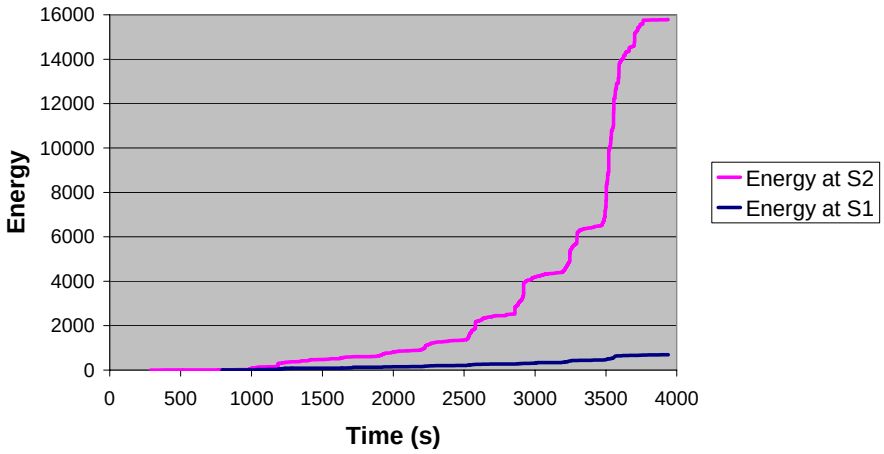

Figure 32 Cumulative stress wave energy trace showing the relative activities at S2 (loading yoke) and S1 (close to desired failure chord). Note also the rapid increase in stress wave activity at S2 indicating that failure is approaching.

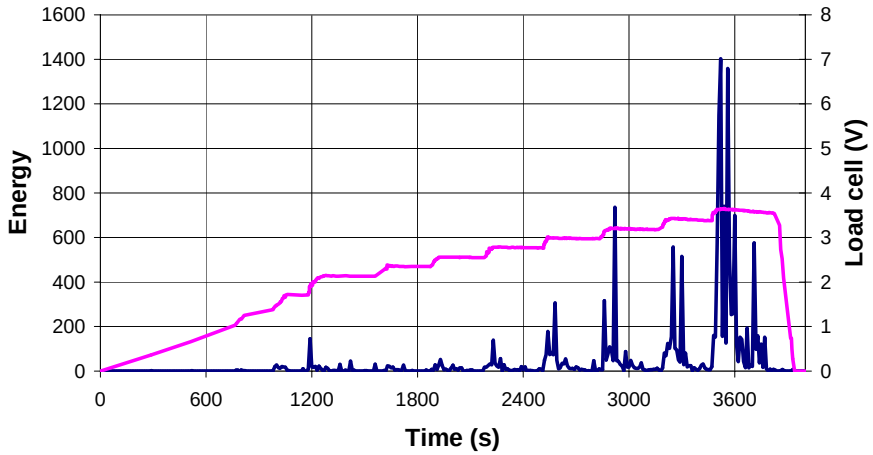

Figure 33 Stress wave activity (blue) detected during step-wise loading of the blade (section 2). The high activity levels and long "die-off" time during load hold indicates the blade is close to failure.

After inspection, the load was reapplied. Loading up to 3.63V again generated far less activity than the first loading (in accordance with the Keiser effect). At load hold for 3.63V however, activity was again registered at Spartan sensor 2. When the load was increased further, the blade failed at the 15.3m loading yoke. Blade failure occurs at 3.88V, thus the final inspection of the blade prior to failure occurred after it had been loaded to 93% (3.63/3.88) of its ultimate strength. This gives far greater possibility of interpreting failure causes and investigating initial damage than only having access to the destroyed structure and attempting to infer causes during a "post-mortem".

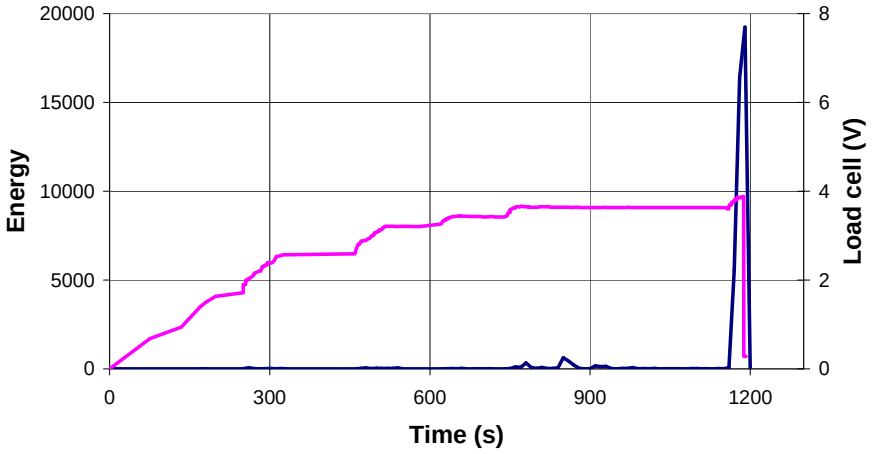

Figure 34 Stress wave activity during the second loading of blade section 2.

The failure of section 2 at the 15.3m loading yoke was unwanted, but as seen in the calculations (simple FE model) prior to the test and the AE readings during the test it was not a surprise. At the moment of failure however the broken blade "sprang back" against the clamping yoke. At this point it was observed that SPARTAN sensor 1 signalled a significant burst of AE activity, where it had previously been relatively inactive. A close inspection of the blade at this area was carried out. It was eventually discovered that lateral cracking inside the central loading spar (x =11m) had been generated and this became significant during the testing of section 3.

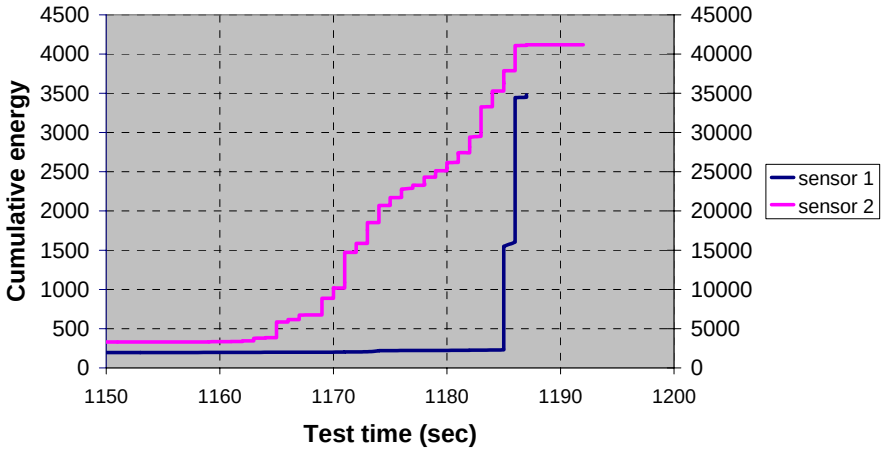

Figure 35 The first y-axis shows cumulated energy detected on S1. The second y-axis shows cumulated energy at S2. S2 shows a "gradual" release of energy typical of composite failure. S1 is almost silent until a sudden burst of energy when the blade "springs back"

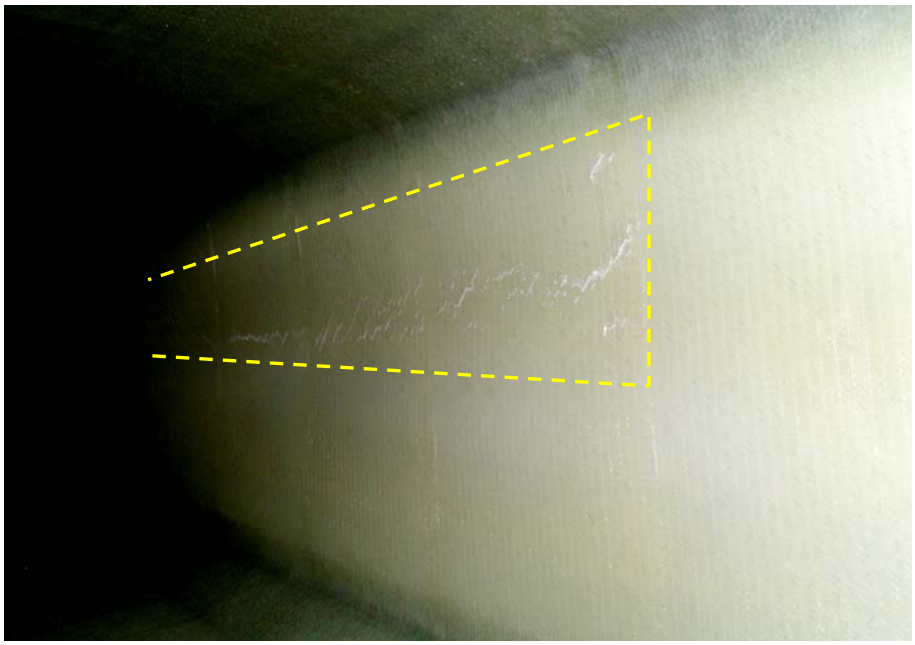

Figure 36 Image taken from inside the central spar showing lateral cracking (enclosed by yellow dashed lines) at approximately 11.3m chord. This damage occurred when the blade "sprang back" against the clamping yoke during section 2 blade failure.

Despite being the simplest loading scheme, the strength calculations predicted most possible failure chord for this test at 4.3m. The LABVIEW sensors were positioned at the 4.5m chord, with one SPARTAN at the 7m chord and the other at the 11.3m loading yoke. The activity levels were very low at the start of the test, followed by a sudden burst of activity at the yoke. Inspection revealed that the lateral cracks caused by the section 2 "back lash" had grown. A second loading was attempted but AE activity at even very low loads warned that the failure would again be this unwanted "yoke damage".

In order to carry out the section 3 test successfully it was decided to make major alterations to the load set-up. The orientation of the blade was changed and

the interior of the blade was reinforced at the 11.3m loading yoke. This successfully prevented the growth of the lateral cracks and permitted load to failure at the 4.5m chord. And once again, the AE activity recorded throughout this loading successfully identified 4.5m as the failure chord in preference to the 7m chord.

5.5 Energy accumulated in the blade

The energy amount absorbed in the blade was calculated for the three tests. The energy amount is simply calculated as the force applied multiplied by the distance it is acting.

The energy absorbed (elastic energy) just prior to failure in the tests was 16kJ for section 1, 86kJ for section 2 and 91kJ for section 3.

It is seen that the energy amount required for the failure of the blade is increasing the closer the root section the failure is located as expected.

6 Conclusion

The test of the 25m Vestas blade showed good results using ultra sonics to scan the blade for irregularities especially in the interface between the relative thin skin laminate and the load carrying main spar. The detection of areas where glue was missing was easy to identify on the basis of the images form the scans.

The method of measuring local deflections of the main spar and skin laminate with the equipment developed in the project seems to be very promising and can be useful for determination of how close the blade is to a failure and for calibration of FE models of blades.

Strain gauge measurements also give good indication of how close the blade is to a failure, i.e. by showing non-linear behavior. The total deflection of the blade does not show clearly a non-linear behavior when the blade is close to a failure.

For large deflections during a static test, it is preferable also to measure the angle by which the load is applied to give the possibility of calculating the real local bending moment.

The practical benefits of the AE monitoring were seen in the three tests These includes identification of unwanted damages at load yokes, identification of damages making it possible to stop test and investigate damage and finally identification of how close you are to failure.

The tests has given a large number of strain gauge measurement, local and global deflection measurements for three different sections of a wind turbine in flapwise load situations up to failure.

The description of all the damages is fully described in [2].

The understanding of how the damages starts up (for example by delamination) is very essential for the strength of the blade and very difficult to decide in a full scale test even though the location of the damages is know by use of acoustic emission sensors. Therefore it is decided, in 2nd phase of this project to investigate a “2D” section of a wind turbine blade, loaded with similar local displacements as found in the full scale test and then in loading and unloading sequences, hopefully describe how damages starts and propagate.

References

[1] Static Test of Vestas blade, V52, Sparkær Center, Confidential

[2] Risø-R-1391(EN)
"Indentification of Damage Types in Wind Turbine Blades Tested to Failure"
Christian P. Debel, AFM
ISBN 87-550-3178-1; ISBN 87-550-3180-3(Internet) ISSN 0106-2840

[3] Risø-R-1393(EN)
"Compression Strength of a Fibre Composite Main Spar in a Wind Turbine Blade"
Find Mølholt Jensen, VEA
ISBN 87-550-3184-6; ISBN 87-550-3185-4(Internet) ISSN 0105-2840

[4] Risø-I-1908(EN)
”V52 Statisk styrke”
Christian Leegaard Thomsen, VEA
Confidential

Title and authors

Full scale testing of wind turbine blade to failure - flapwise loading

Erik R. Jørgensen, Kaj. K. Borum, Malcolm McGugan, Christian L. Thomsen, Find M. Jensen, Christian P. Debel og Bent F. Sørensen

ISBN	ISSN
87-550-3181-1 87-550-3183-8 (Internet)	0106-2840

Department or group	Date
VEA/VIM	16.06.2004

Groups own reg. number(s)	Project/contract No(s)
	ENS-1363/01-0007

Sponsorship

Danish Energy Authority, the Ministry of Economics and Business Affairs

Pages	Tables	Illustrations	References
29	0	36	4

Abstract (max. 2000 characters)

A 25m wind turbine blade was tested to failure when subjected to a flapwise load. With the test setup, it was possible to test the blade to failure at three different locations.
The objective of these tests is to learn about how a wind turbine blade fails when exposed to a large flapwise load and how failures propagate.
The report shows also results from ultra sonic scan of the surface of the blade and it is seen to be very useful for the detection of defects, especially in the layer between the skin laminate and the load carrying main spar.
Acoustic emission was successfully used as sensor for the detection of damages in the blade during the test.
The report contains measurements of the total deflection of the blade, the local deflection of the skin and the load carrying main spar and also measurement of strain all as a function of the applied load and up to failure of the blade.
The “post mortem” analysis and description of how the damages propagate during the tests are reported in a separate report

Descriptors INIS/EDB